SAKARYA UNIVERSITY JOURNAL OF COMPUTER AND INFORMATION SCIENCES
http://saucis.sakarya.edu.tr/
e-ISSN: 2636-8129
Publisher: Sakarya University
Vol. 7, No. 2, 2024, 217-226
DOI: 10.35377/saucis...1463788
SAUCIS
SAKARYA UNIVERSITY

RESEARCH ARTICLE

Classification of Solar Cells EL Images with Different Busbars Via Deep Learning Models

Miktat Aktaş[1], Ferdi Doğan[2], İbrahim Türkoğlu[3]

[1] GTC GUNES SAN. ve TIC. A.S./R&D Center, Adıyaman, Türkiye
[2] Adıyaman University, Computer Engineering, Adıyaman, Türkiye
[3] Fırat University, Software Engineering, Elazığ, Türkiye

Corresponding author:
Miktat Aktaş, GTC GUNES SAN. ve TIC. A.S./R&D Center, Adıyaman, Türkiye
mkttkts@gmail.com

Article History:
Received: 03.04.2024
Accepted: 03.06.2024
Published Online: 26.08.2024

ABSTRACT
Electricity generation from renewable energy sources such as solar energy has come to the forefront in the last decade. The solar energy cell is an indispensable part of the solar energy ecosystem of solar panels, and defective cells cause financial losses in energy production. Experienced experts are needed to detect defects on solar cells. Autonomous systems are important to accelerate the process. Classical image processing techniques are used to manually detect defects on cells. To use these techniques, many parameters are need to be entered into EL imaging software. However, in this study, these processes were carried out automatically without the need for external intervention. False detection/classification may occur during the processes performed by EL imaging devices due to weakness of the operator experience or EL imaging software. It is aimed to use automatic image processing and then deep learning techniques to achieve faster and higher performance than the results obtained from EL imaging devices using classic image processing techniques. AI algorithm and deep learning models can be an important solution. In this study, two AI algorithm and 10 different deep learning models were used to classify solar cells. EL images of defective and normal solar cells with 4 and 5 busbars were used in the study. The dataset, includes 9360 images of solar cells, 4680 of which are defective and 4680 are normal. Performance evaluation of the models made according to the confusion matrix. According to the results, Mobilenet-v2 and VGG-19 achieved the highest validation accuracy rate of 99.68%. According to F1-score, Mobilenetv2 achieved the highest performance of 99.73%. It has been shown that the Mobilenet-v2 is slightly more successful than other models in terms of validation and F1-score. The results show that trained DL models can be used as an inspection method in the production line of solar panels and cells.

Keywords: Solar cells, Deep learning, Image processing, EL Image, Defects

1. Introduction

Electricity generation from solar panels has been very popular recently, just like artificial intelligence-supported systems. The quality of solar cells, which is the most important element of the solar panel and determines the maximum electricity production capacity, power and performance, is undoubtedly very important for manufacturers and users. For this purpose, many defects detection and classification equipment/processes are used during solar cell/panel production and after panel installation on solar plants. Determination of cell defects from Electrolumnesans (EL) images is one of these methods. In EL imaging, it is possible to detect cell defects, especially in PV panels. Cell defects appear as dark lines on the solar cell in the EL image. Especially in multicrystalline solar cells, crystallographic defects typically appear as dark lines. Cell cracks are detected by a person trained to recognize cell cracks in PV cells and panels. A well-trained person can detect cracks by looking at the EL image of a solar panel. [1]

As shown in Figure 1, the classic EL imagining test is conducted in a dark environment by applying reverse current to the PV solar panel and the reflected photons are captured by the CCD (Charge Coupled Device) camera; the images similar to radiology results as in Figure 2. The captured image can be interpreted only by experts as in radiology results. EL images are controlled by an expert, and if s/he detects any defects in cells, these cell strings must be replaced with non-defective cell strings before the lamination process. Therefore, manual classification and inspection may cause a waste of time and some misclassification problems. Especially during solar cell/panel production, classification of the cell defects is quite helpful for quality & inspection processes.

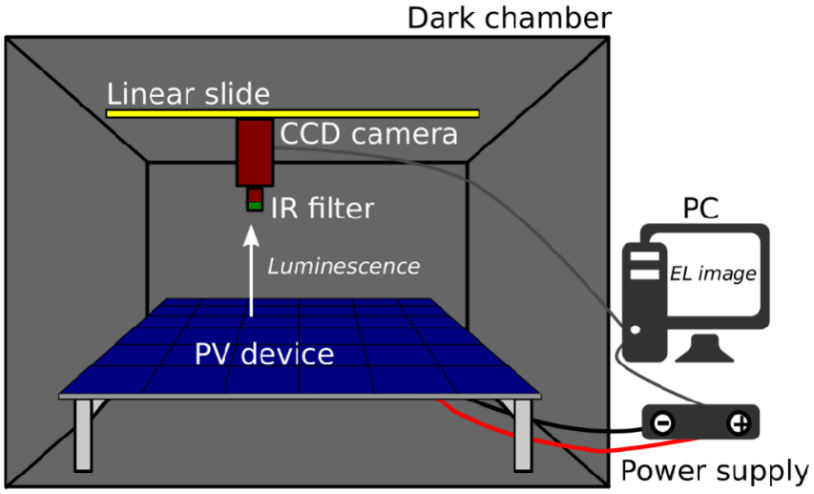

Figure 1. EL Imaging Technique Representation [2]

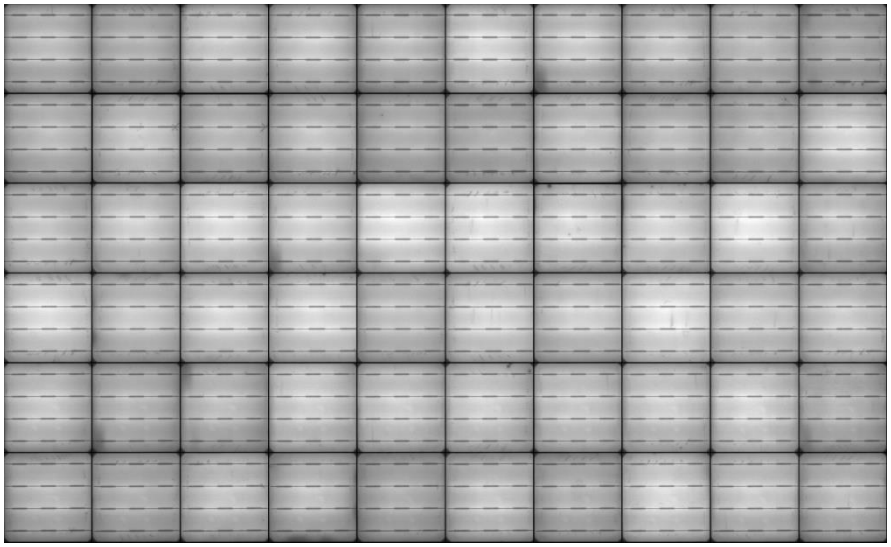

Figure 2. EL Image of 60 Cells PV Solar Panel

The Classic EL imaging software segments the image consisting of 60 or 72 cell images according to the parameters entered by the operators and writes the evaluation result of each cell to an XML file. In some cases, due to parameter or operator-related reasons, false cell segmentation may occur as shown in Figure 3.

Figure 3. False Segmented Solar Cell

There are some cell defect types like micro-cracks, finger interruptions, material defects, Finger Interruptions, Cell Inter-connection Problems shown in Figure 4. Each defect type impacts panel performance differently; even a combination of several may result in negligible effect. In some cases, depending on the size and number of defects may cause a panel performance loss of up to 60% [3]

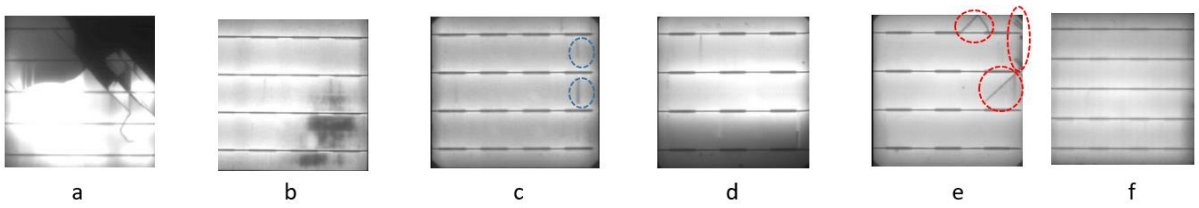

Figure 4. Types of Defects and Normal Cells in the Dataset.

a) Electrically Insulated Cell Parts b) Material Defects c) Finger Interruptions d) Cell Inter-connection Problems e)Microracks f)Cell without any defects(Normal)

The images obtained from the EL device are presented to the expert using classical image processing techniques. The expert examines the images from the EL device and manually detects cell damage in the image.

Using deep learning models for inspection of EL images, it will provide minimizing the faulty detections caused by the operator and the machine, reducing the time spent for damage detection to less than 1'min and to carry out the process in a healthy way without the need for an operator at the station.

Deep learning models used in the study, the arrangement and branching of the DL(Deep Learning) layers are differ. A sample architecture showing the layers used in deep learning models is shown in Figure 5.

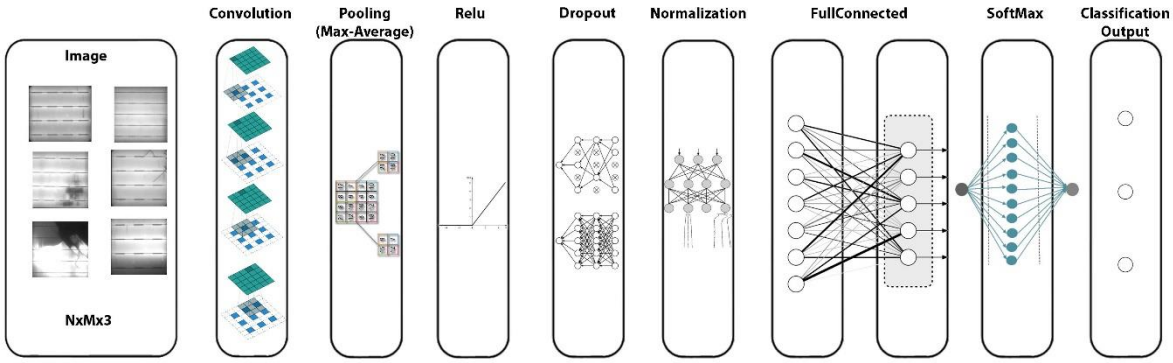

Figure 5. Sample Layer Structure Used in DL Models for Classification Problems[4]

A dataset consisting of defective and normal cells, the input image in Figure 5, is put as input data to a sample DL model. Then, feature extraction is performed via the convolutional layer. In the next layers, the image size used as input for the network is reduced by the polling process. Relu is used for the activation function. The probability of memorization of the network is reduced, and some of the random weights in the network are discarded in the dropout layer. The image data is standardized via the normalization layer. In a fully connected layer, every neuron makes connections to all neurons in the prior layer. This allows the network to integrate the local features extracted earlier, like edges and shapes, into a bigger picture, ultimately recognizing complex patterns across the entire image. The Softmax layer is the entropy layer and it makes probabilistic estimation and estimates which class the input image belongs to via the Classification layer, [5]

This study used 10 Deep Learning CNN(Convolution Neural Network) models, which have different numbers and types of layers for cell classification. These models are Mobilenetv2, Darknet19, Darknet53, Alexnet, Googlenet, Vgg16, Vgg19, Resnet50, Resnet-101, Densenet201. In addition to these DL models we used classic AI(Artificial Intelligence) algorithms as SVM(support Vector Machine) and KNN(K-Nearest Neighbor). In this way, it will be possible to see which model achieve more successful results and this study will guide the researchers who work in this field. The dataset used in this study was selected and validated from a real production line and by experienced engineers. In addition, the Confusion matrix was used as a measure of the success of the models and precision, accuracy, sensitivity, and F1-score parameters were used.

In the introduction section, information about cell defect classification using classical image processing techniques is given and what can be done with the use of AI is briefly explained. In 2 related studies, previous studies for the detection of cell damage and the methods used in these studies are stated in detail. The 3 material and method sections mention the method we used in our study and how the study progressed. In the results section 4, the results we obtained with different deep learning models in our study are explained. The results and evaluation were made in 5 discussion sections. In the 6 discussion sections, there are discussions about the results obtained.

2. Related Work

In 2021, we studied crack detection on the solar cell by using the Alex-Net DL model in the dataset we had created ourselves. According to the results we gained from the study, we achieved the detection of cracks in solar cells with an accuracy of 79.40%. [3]

In Table 1, related to the studies listed that were classified as defect/undefect, the common feature of all of them was that the number of images used in the dataset and the number of cell defects were limited, An imbalanced dataset had been used in some researches [6][7]to get the most accurate result we had created and used a dataset that is balanced, much larger and included more defect types. At the same time, it achieved the highest result in metrics such as Accuracy, Recall, Precision, and F-1 score. Besides, 10 different DL models and 2 traditional AI were used for training and testing. Lastly, Alaa S. Al-Waisy studied on two different datasets their class numbers are unbalanced. To overcome this situation, they use some data augmentation techniques. They also trained and tested the datasets by pre-trained and hybrid model and get highest performance with the hybrid model [8].

Lee et all,developed a deep learning architecture called LIRNET(Local Integral Regression Network) for a dataset of 20000 infrared images and 12 classes and performed classification in 2 phases. The dataset is unbalanced like the dataset used in other studies, and they achieved an 89% accuracy rate with the used architecture [9].

Deitsch S. et al, studied on a limited number of dataset and try to automatic segmentation in both defect and normal cell images and they get F1 score as 97.23%[10]. Akram Waqar et al, studied on same dataset of Deitsch S. et al, they classify the dataset as defect and not defect and get 92.80% Accuracy rate [11].

Amirul Anwar S. et al, studied with a very limited dataset and they classify the dataset as defect and not defect and get 83.89% Accuracy rate[12]. Bartler A. et al, studied with a relatively large dataset and classify the dataset as defect and good and get 87.04% Recall rate [13]. Wang J. et al, studied with two different datasets and classified the dataset as defective and normal and get a 96.17% Accuracy rate [14]

In Table 1, related research is listed with the researcher's name, number of classifications, dataset size and test results in terms of Accuracy, Recall, Precision and F1-score.

Table 1. Related Works

Studies	Classification	Number of Total El Images	Accuracy	Recall	Precision	Highest F-1 Score
Balzategui J. et al [6]	Defect vs Not Defect	542	-	0.920	0.850	0.883
Balzategui J.et al[7]	Defect vs Not Defect	542	-	0.875	0.823	0.847
Waqar Akram M. et al [11]	Defect vs Not Defect	2624	0.928	0.920	0.93	0.9249
Amirul Anwar S. et al[12]	Defect vs Not Defect	600	0.8389	0.971	-	-
Bartler A. et al [13]	Defect vs Good	98280		87.04		
Wang J. et al. [14]	Defective vs Normal	2223 & 5991	0.9617	0.9516	0.9603	0.9557

The differences between classical image processing techniques and artificial intelligence studies are included in the related studies section. Here, it has been seen that studies carried out with deep learning models, one of the artificial intelligence techniques, have achieved successful results in damage detection. It is thought that this study, conducted to fill the gap in this subject, contains important findings that will contribute to the literature.

3. Material and Method

a. Requirement

Cracked or damaged solar cells cause efficiency loss in production and, consequently an increase in production costs. Micro cracks and defects not only reduce cell productivity in that area but also reduce cell reliability. [1]

A damaged cell or group of cells may cause hot-spot heating problems when the operating current in a panel exceeds the reduced short-circuit current of the fault cell. the cell is forced into reverse current and must dissipate this accumulated power. Indeed, if the dissipation force is large enough, this reverse-polar cell can overheat and melt the solder or cause the back sheet to deteriorate (Figure 6). Hot-spot cells show low parallel resistance when reverse current performance is limited by current, or high parallel resistance when reverse current performance is limited by voltage. In either case, the cell may experience hot-spot problems in different ways.[15]

Each cell defects have different impacts; for instance, dark area causes reduced power output immediately, while microcracks may leads a reduced power output in the future. Because, many operators of solar production line wish an automated detection of defect cells and a further classification of defect cells into various defect categories to decide which solar modules must to be replaced immediately or in the future. [13]

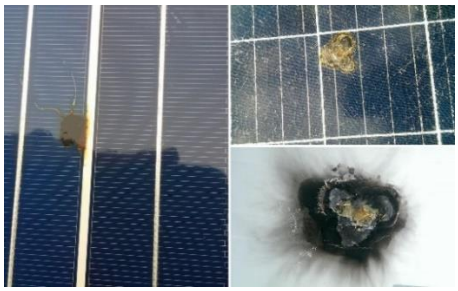

Figure 6. Hotspot's Effect on Solar Panel [15]

b. Method

As shown in Figure.7 First, firstly we extracted cell images from 72- or 60-cell panel EL images manually (manually means that we didn't use any AI methods for this process instead we have gathered the dataset among 200.000 cell images' by C# based software which we designed and coded. The software firstly import images metadata stored in xml file to sql database then filter defective cells according to this data.), all images had gathered from the EL machine used in the production line, then experts identified and labeled the defect cells from images. Sufficient defect and normal cells were collected for the dataset, 9260 EL images. 80% of the images were used for training and 20% for testing. 10% of the images used for training were also used for validation. The training and test images selected in the study are taken randomly. The training and test images in the model are automatically generated from the dataset. Then, various deep learning models were trained with this dataset and tested. At the same time, alexnet-based feature extraction method used for SVM and KNN, then classification made with these classic AI algorithms. Fully connected layer named as 'fc6' feature extraction layer used. The results were compared each other and the most successful deep learning model was determined using the confusion matrix and metrics gathered from the matrix.

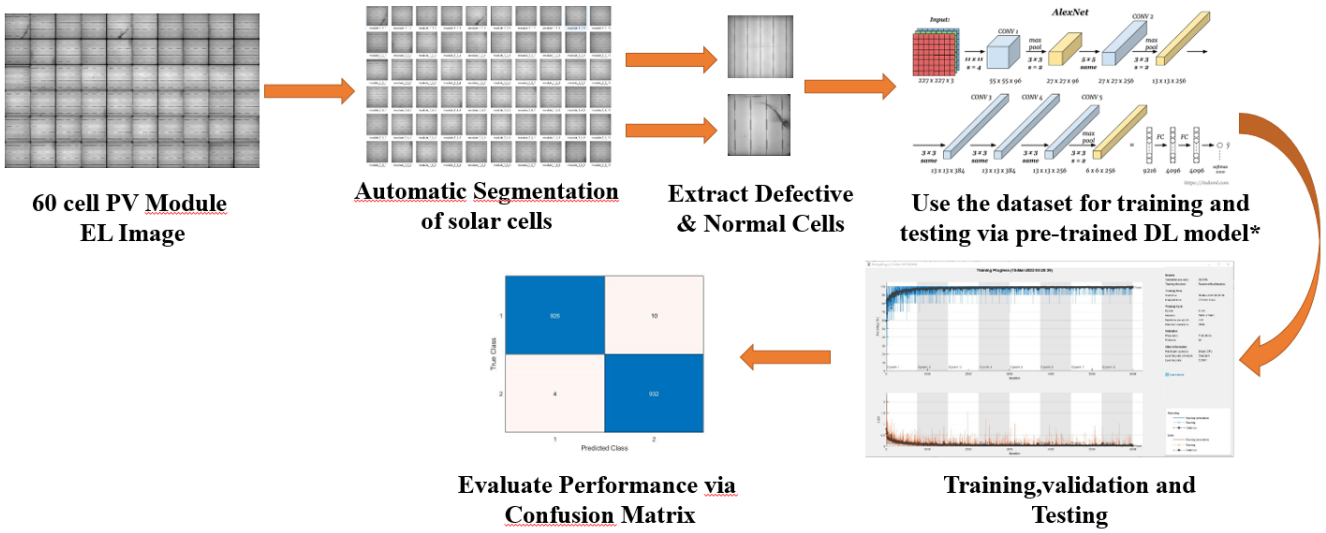

Figure 7. Flow Chart for Solar Cells Classification ,*[16]

c. Dataset

There are 9360 EL images with high resolution of solar cells, 4680 of which are defective (Electrically Insulted cell parts, microcracks, material defect, finger interruption, cell interconnection problems), as shown in Figure 4, and 4680 are non-defect. Each cell size in the panel varies between 950x960-930x850. The reason for the different cell sizes is that the panel images were taken in different sizes. Some panels contain 72 solar cells while some panels consist of 60 solar cells. As shown in Figure Figure 8, 41% of solar cell images have 5 busbars, and 59% have 4 busbars. The image resolutions were adjusted according to the required input size of the DL models before training. The dataset is separated randomly for training and testing. 80% (7488 images) of the dataset was used for training, %10 of the reserved dataset for training was used for validation and the remaining 20% (1872 images) for testing.

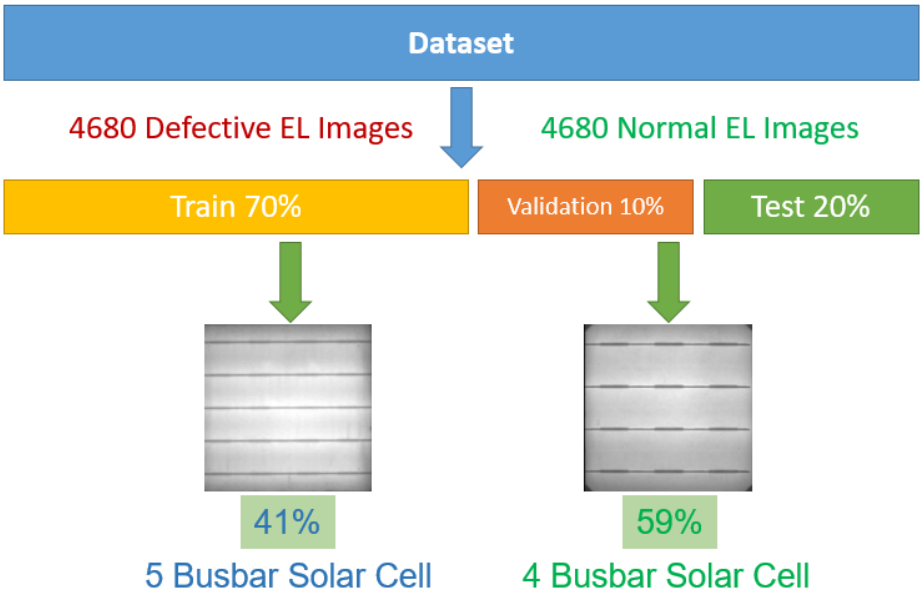

Figure 8. Dataset Features

d. Data Augmentation

Although there are enough samples in the data set, we used the data augmentation technique, as shown in Figure 9, to reduce the possible overfitting and to obtain more precise results. [17]

RandRotation: Range of rotation, in degrees, applied to the input image. RandRotation value was [90,90]

RandXReflection: Random reflection in the left-right direction, specified as a logical scalar. When RandXReflection is true (1), each image is reflected horizontally with a 50% probability. When RandXReflection is false (0), no images are reflected. RandXReflection value was true (1)

RandYReflection: Random reflection in the top-bottom direction, specified as a logical scalar. When RandYReflection is true (1), each image is reflected vertically with a 50% probability. When RandYReflection is false (0), no images are reflected. RandYReflection value was true (1)

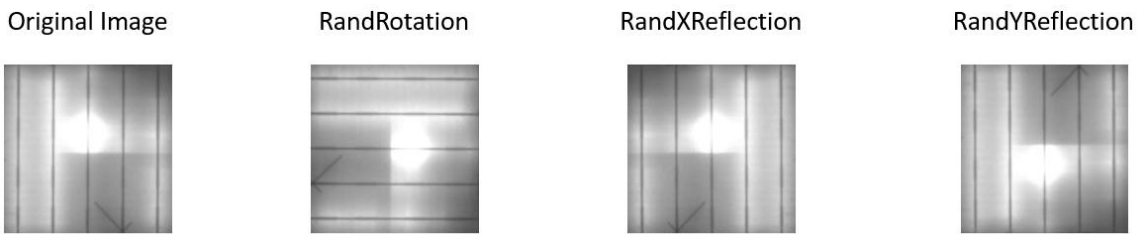

Figure 9. Data Augmentation Techniques

e. Deep Learning Models

As can be seen in Table 2, training and tests were carried out with 10 different deep learning models, apart from SVM and KNN classical artificial intelligence algorithms. Feature extraction for SVM and KNN algorithms was done by Alexnet. Darknet19 and Darknet53 models, used as backbones in YOLOv2 and YOLOv3 algorithms, which perform real-time object detection, are also used for classification. Features such as layer, depth and parameter of the models are given in the table.

Table 2. Features of Used DL Models [5]

Model	Input Size	Number of Layers	Number of Connections	Depth	Number Of Parameters	Top-1 Error rate	Top-5 Error rate
AlexNet	227x227	25	-	8	61m	36.7	15.4
VGG16	224x224	41	-	16	138m	25.6	8.1
VGG19	224x224	47	-	19	144m	25.5	8
GoogleNet	224x224	144	170	22	4m	-	6.67
Mobilenet-v2	224x224	154	164	53	3.47 m	28.2	9.0
ResNet50	224x224	177	192	50	25.6m	22.8	6.71
ResNet101	224x224	347	379	101	44.6m	21.75	6.05
Darknet-19	256x256	64	63	19	5.58 m	22.9	6.3
Darknet-53	256x256	184	206	53	40.5 m	22.8	6.2
DenseNet201	224x224	708	805	201	20m	21.46	5.54

Training and testing of models were done on the Matlab 2019b platform. Training options were selected as below;

SolverName: SGDM (Stochastic Gradient Descent with Momentum), MiniBatchSize:128, MaxEpochs:20, InitialLearnRate:1e-3, Shuffle:Every-epoch, ValidationFrequency:50, Verbose:False.

f. Evaluation Performance of Deep Learning Models

Each model was trained and tested with the same images. A confusion matrix was used for the evaluation of the performance of the DL models, and Accuracy, Sensitivity, Precision and F1-score metrics derived from this matrix were used for the final evaluation. The formulas for these metrics are below.

Predicted Values \ Actual Values	Positive	Negative
Positive	TP	FP
Negative	FN	TN

TP: The number of defect cells which are defect in reality, that the DL model has found,

FP: The number of defect cells which are non-defect in reality, that the DL model has found,

FN: The number of non-defect cells which are defect in reality, that the DL model has found,

TN: The number of non-defect cells which are non-defect in reality, that the DL model has found,

i. Accuracy:

Accuracy gives the proportion of the total number of predictions that were correct as shown in Eq.1: [18]

$$\boldsymbol{Accuracy} = \frac{(TP + TN)}{(TP + FN + FP + TN)} \quad (1)$$

ii. Sensitivity:

Sensitivity, recall, or the TP rate (TPR) is the fraction of positive values out of the total actual positive instances (i.e., the proportion of actual positive cases that are correctly identified) as shown in Eq.2::

$$\boldsymbol{Sensivity(Recall)} = \frac{TP}{(TP + FN)} \quad (2)$$

iii. Precision:

Precision or the positive predictive value, is the fraction of positive values out of the total predicted positive instances. In other words, precision is the proportion of positive values that were correctly identified as shown in Eq.3:

$$\textbf{Precision} = \frac{TP}{(TP + FP)} \quad (3)$$

iv. F1 score:

The F1 score, F score, or F measure is the harmonic mean of precision and sensitivity. It gives importance to both factors as shown in Eq.4 [17]

$$\mathrm{F-Score} = 2 * \frac{(\mathrm{Precision} * \mathrm{Recall})}{(\mathrm{Precision} + \mathrm{Recall})} \quad (4)$$

4. Results

In our study, since the training of the models was done on different computers and the features of these computers were different, a comparison was not made according to the working time, but the working time values are given in Table 3. As can be seen in the same table, the validation values obtained during the training were consistent with the test results in Table 4. The highest Validation Accuracy value was obtained with Mobilenet-v2 and Vg-19 models.

Table 3. Validation Accuracy and Runtime of DL models

Name	Validation Accuracy	Runtime (Min.)
Mobilenet-v2	0.9968	229.15
Darknet19	0.9957	239.12
Darknet53	0.9963	636.29
Alexnet	0.9893	20.14
Googlenet	0.9936	118.47
Vgg16	0.9909	52.8
Vgg19	0.9968	57.5
Resnet50	0.9936	29.24
Resnet101	0.9952	58.7
Densenet201	0.9963	636.29

The detailed test results of DL Models and Svm & Knn Classic AI Algorithms are listed in Table 4. There are the number of TP (True Positive), FP (False Positive), FN (False Negative), and TN (True Negative) predictions of the models and Precision, Sensitivity, Accuracy and F-score metrics which are derived from the predictions. The formula of these metrics is given under the "Evaluation Performance of Deep Learning Models" section.

The graphics of the training performed by the models with the dataset are shown in Figure 10. Each model's training and processing process according to the epoch is given.

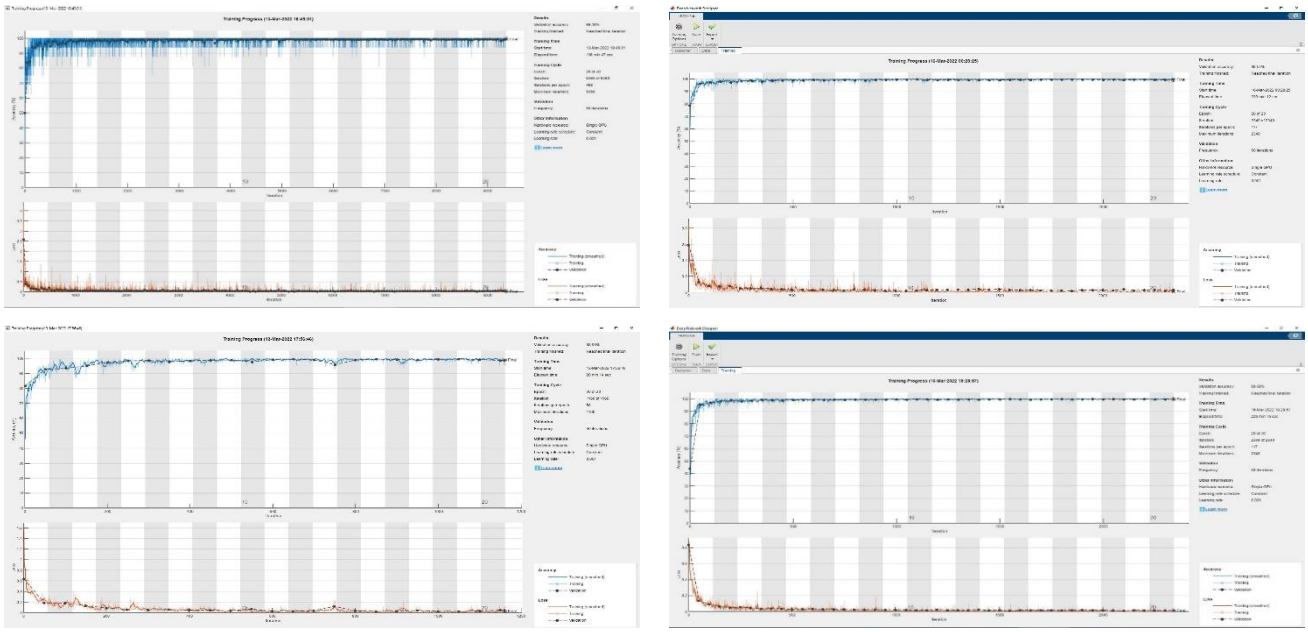

Figure 10. Training Deep Learning Models

According to the results in Table 4, Mobilenet-v2 and VGG-19 achieved the highest validation accuracy rate of 99.68%. According to F1 scores, Mobilenetv2 achieved the highest performance of 99.73%. It has been shown that all DL models show high performance for classification of defect and non-defect solar cells especially Mobilenet-v2 is more successful than other models in accuracy and F1-score by a very small margin.

Table 4. Performance of DL models & Classic AI Algorithms

Name	TP	FP	FN	TN	Precision	Sensitivity	Accuracy	F-score
Mobilenet-v2	**934**	**3**	**2**	**933**	**0.9968**	**0.99786**	**0.99733**	**0.99733**
Darknet-19	931	4	5	932	0.99572	0.99466	0.99519	0.99519
Darknet-53	930	1	6	935	0.99893	0.99359	0.99626	0.99625
Alexnet	930	15	6	921	0.98413	0.99359	0.98878	0.98884
Svm	910	9	26	927	0.99021	0.97222	0.9813	0.98113
Knn	834	13	102	923	0.98465	0.89103	0.93857	0.9355
Googlenet	926	4	10	932	0.9957	0.98932	0.99252	0.9925
Vgg16	927	3	9	933	0.99677	0.99038	0.99359	0.99357
Vgg19	935	7	1	929	0.99257	0.99893	0.99573	0.99574
Resnet50	925	3	11	933	0.99677	0.98825	0.99252	0.99249
Resnet101	931	1	5	935	0.99893	0.99466	0.99679	0.99679
Densenet201	932	2	4	934	0.99786	0.99573	0.99679	0.99679

Apart from these results, it is clearly understood that SVM and KNN algorithms perform quite well, of course, it is seen that SVM achieves higher scores than KNN.

5. Conclusion

In this study, for all performance parameters (Precision, Recall, F-score) we get the highest results among the previous studies. The reason for the higher performance than previous studies is thought to be the smaller data set sizes used in previous studies and the correct distinction between defect and non-defect cells. Another reason is that although the data set size is sufficient, high results were obtained due to data augmentation techniques. Another feature of this study compared to previous studies is the use of cells with different numbers of busbars in the data set. In this study both AI algorithms and deep learning models were tested and compared. High F-Score and Accuracy results of the DL models show defective & normal solar cells can be classified with deep learning successfully. For the next step defective cells in the Dataset will be separated according to their type then will be classified via the DL models and a new DL model which we will design and develop and compare its performance to pre-trained models. If the accuracy or F-score ratio is less than 90%, preprocessing methods will be implemented to improve the ratio.

6. Discussion

It is seen that deep learning models perform quite successfully in the classification of defects in solar cells. Replacing the classical image processing techniques used currently in EL devices with a defect classification system prepared with deep learning models will produce very economical results for solar energy panel manufacturers. The system to be integrated into EL devices will enable the process to be done automatically without requiring an expert. This once again reveals the importance and requirement of the study. The high performance rate obtained from the models may be due to the fact that the dataset consists of two classes. The results that will occur if the number of classes is large will be revealed in subsequent studies. Consisting of two classes containing defect and normal images constitute the boundaries of the study. In future studies, it is planned to work on datasets with a larger number of classes. The training process of deep learning models reveals their performance. However, it appears that it is not overfitting.

References

[1] M. Abdelhamid, R. Singh, and M. Omar, "Review of microcrack detection techniques for silicon solar cells," *IEEE Journal of Photovoltaics*, vol. 4, no. 1. pp. 514–524, Jan. 2014. doi: 10.1109/JPHOTOV.2013.2285622.

[2] K. G. Bedrich, "Quantitative electroluminescence measurements of PV devices," Loughborough University, 2017.

[3] M. Aktas, F. Doğan, and İ. Türkoğlu, "Analysis Of Cracks In Photovoltaic Module Cells From Electroluminescence Images By Deep Learning.," in *1st International Conference on Computing and Machine Intelligence*, 2021, pp. 103–103.

[4] F. Doğan and İ. Türkoğlu, "Derin Öğrenme Modelleri ve Uygulama Alanlarına İlişkin Bir Derleme," *Dicle Üniversitesi Mühendislik Fakültesi Mühendislik Derg.*, vol. 10, no. 2, pp. 409–445, 2019, doi: 10.24012/dumf.411130.

[5] F. Doğan and I. Turkoğlu, "Comparison of deep learning models in terms of multiple object detection on satellite

images," *J. Eng. Res.*, Nov. 2021, doi: 10.36909/jer.12843.
[6] J. Balzategui *et al.*, "Semi-automatic quality inspection of solar cell based on Convolutional Neural Networks," in *2019 24th IEEE International Conference on Emerging Technologies and Factory Automation (ETFA)*, IEEE, Sep. 2019, pp. 529–535. doi: 10.1109/ETFA.2019.8869359.
[7] N. A.-A. Julen Balzategui, Luka Eciolaza, *2020 IEEE/SICE International Symposium on System Integration (SII)*. 2020.
[8] A. S. Al-Waisy *et al.*, "Identifying defective solar cells in electroluminescence images using deep feature representations," *PeerJ Comput. Sci.*, vol. 8, p. e992, 2022.
[9] S.-H. Lee, L.-C. Yan, and C.-S. Yang, "LIRNet: A lightweight inception residual convolutional network for solar panel defect classification," *Energies*, vol. 16, no. 5, p. 2112, 2023.
[10] S. Deitsch *et al.*, "Automatic Classification of Defective Photovoltaic Module Cells in Electroluminescence Images," Jul. 2018, doi: 10.1016/j.solener.2019.02.067.
[11] M. W. Akram *et al.*, "CNN based automatic detection of photovoltaic cell defects in electroluminescence images," *Energy*, vol. 189, Dec. 2019, doi: 10.1016/j.energy.2019.116319.
[12] S. A. Anwar and M. Z. Abdullah, "Micro-crack detection of multicrystalline solar cells featuring an improved anisotropic diffusion filter and image segmentation technique," *Eurasip J. Image Video Process.*, vol. 2014, 2014, doi: 10.1186/1687-5281-2014-15.
[13] A. Bartler, L. Mauch, B. Yang, M. Reuter, and L. Stoicescu, "Automated Detection of Solar Cell Defects with Deep Learning," in *2018 26th European Signal Processing Conference (EUSIPCO)*, IEEE, Sep. 2018, pp. 2035–2039. doi: 10.23919/EUSIPCO.2018.8553025.
[14] J. Wang *et al.*, "Deep-Learning-Based Automatic Detection of Photovoltaic Cell Defects in Electroluminescence Images," *Sensors*, vol. 23, no. 1, p. 297, Dec. 2022, doi: 10.3390/s23010297.
[15] J. Wohlgemuth and W. Herrmann, "Hot spot tests for crystalline silicon modules," in *Conference Record of the Thirty-first IEEE Photovoltaic Specialists Conference, 2005.*, 2005, pp. 1062–1063.
[16] V. Tiwari and S. C. Jain, "An optimal feature selection method for histopathology tissue image classification using adaptive jaya algorithm," *Evol. Intell.*, vol. 14, no. 3, pp. 1279–1292, Sep. 2021, doi: 10.1007/s12065-019-00205-w.
[17] "ImageDataAugmenter,." Accessed: May 19, 2023. [Online]. Available: https://www.mathworks.com/help/deeplearning/ref/imagedataaugmenter.html
[18] D. K. Sharma, M. Chatterjee, G. Kaur, and S. Vavilala, "Deep learning applications for disease diagnosis," in *Deep Learning for Medical Applications with Unique Data*, Elsevier, 2022, pp. 31–51. doi: 10.1016/B978-0-12-824145-5.00005-8.

Author(s) Contributions
Miktat AKTAŞ: Conceived and designed the analysis, Collected the dataset, contributed data or analysis tools, Performed the analysis, Writing the paper
Ferdi DOĞAN: Contributed data or analysis tools, Performed the analysis, Writing the paper
İbrahim TÜRKOĞLU: Conceived and designed the analysis, contributed data or analysis tools, Performed the analysis

Acknowledgments
This study is funded by GTC Gunes Sanayi and Ticaret A.S. I am very grateful to CEO of GTC Gunes Sanayi ve Ticaret A.S, Ayşe Çiğdem BESEN for her permission to use required dataset and her support during my studies.
This study/work was presented in the 3rd International Conference on Photovoltaic Science and Technologies (PVCon2022) held on July 5-7, 2022 in Middle East Technical University (Ankara, Turkey)
This this study was supported by Scientific and Technological Research Council of Turkey (TUBITAK) under the Grant Number 123E697 The authors thank to TUBITAK for their supports

Conflict of Interest Notice
Miktat AKTAŞ, Ferdi DOĞAN and İbrahim TURKOGLU declare that there is no conflict of interest regarding the publication of this paper.

Support/Supporting Organizations
This study is supported by GTC Gunes Sanayi and Ticaret A.S

Plagiarism Statement
This article has been scanned by iThenticate ™.